Towards validation of diffusion MRI tractography: bridging the resolution gap with 3D Polarized Light Imaging

Abib Alimi, Samuel Deslauriers-Gauthier, Rachid Deriche

Towards validation of diffusion MRI tractography: bridging the resolution gap with 3D Polarized Light Imaging

Abib O. Y Alimi[1], Samuel Deslauriers-Gauthier[1], and Rachid Deriche[1]

[1]*Athena Project-Team, Inria Sophia Antipolis Méditerranée, Université Côte d'Azur, Sophia Antipolis, France*

Synopsis

Three-dimensional Polarized Light Imaging (3D-PLI) is an optical approach presented as a good candidate for validation of diffusion Magnetic Resonance Imaging (dMRI) results such as orientation estimates (fiber Orientation Distribution Functions) and tractography. We developed an anlytical approach to reconstruct fiber ODFs from 3D-PLI datasets. From these fODFs, here we compute brain fiber tracts via dMRI-based probabilistic tractography algorithm. Reconstructed fODFs at different scales proves the ability to bridge the resolution gap between 3D-PLI and dMRI, demonstrating, therefore, a great promise to validate diffusion MRI tractography thanks to multi-scale fiber tracking based on 3D-PLI.

Introduction

Three-dimensional Polarized Light Imaging (3D-PLI) is an optical technique that utilizes the birefringence in postmortem organs (brain/heart) to map their spatial fiber structure at a submillimeter resolution[1-3]. It provides us with high-resolution tissue fiber orientation estimates from which different approaches have been based to reconstruct fiber orientation distribution functions (ODF)[4-6]. This study focuses on our analytical fiber ODF approach to present tractography at different spatial resolutions from 3D-PLI human brain datasets.

Methods

Analytical fiber ODF in 3D-PLI: Different methods have been proposed to reconstruct the fiber ODF from high-resolution 3D-PLI datasets[4-6], based on the important concept of super-voxel to downsample the micrometer resolution orientation data. A super-voxel is composed of K *native voxels*[4] containing each a single high-resolution tissue fiber orientation. In the analytical approach, we define each tissue fiber orientation as a 2D Diracs delta δ function on the unit sphere and the fiber ODF f as a weighted sum of the K Diracs in a given super-voxel[6]

$$f(\theta,\phi) = \frac{1}{K}\sum_{k=1}^{K} w_k \delta(\cos\theta - \cos\theta_k)\delta(\phi - \phi_k)$$

where w_k are the weights and the K parameters (θ_k, ϕ_k) completely characterize the fODF $f(\theta,\phi)$. This later is then analytically described on a truncated spherical harmonics (SH) basis as $f(\theta,\phi) \approx \sum_{l=0}^{l_{max}} \sum_{m=-l}^{l} c_{lm} Y_l^m(\theta,\phi)$ with l_{max} being the maximum order or bandlimit of the truncation and c_{lm} the SH coefficients elegantly and efficiently computed via the spherical Fourier transform[7] by means of the Diracs

$$c_{lm} = \frac{1}{K}\sum_{k=1}^{K} w_k \overline{Y_l^m}(\theta_k,\phi_k)$$

.

Note that this approach is independent of the SH basis used and here the real and symmetric basis[8] is considered.

Fiber-tracking at multiple resolutions: The use our fODF computation method allows to integrate K high-resolution tissue fiber orientations from native voxels into a super-voxel. By changing the super-voxel size, we navigate through the spatial scales and thus compute fiber tracks or streamlines at different resolutions. We performe fiber-tracking using the MRtrix3 package (www.mrtrix.org) and probabilistic streamlines via the 2nd order integration over fibre orientation distributions (iFOD2) algorithm[9].

Human brain dataset: The 3D-PLI human dataset consists of a set of coronal slices from the right hemisphere and is fully described in [10]. Each section has a pixel size of 64 × 64 μm^2 and a 70 μm thickness. The super-voxel which closes the gap with diffusion MRI resolution has a size of 30 × 30 native voxels in the xy-plane and 2 voxels in the z-axis corresponding to a set of two slices. For this preliminary study, only 10 brain sections have been processed so far, thus the resolution in the z-axis is 0.14 mm while in the xy-plane, it is 1.92 × 1.92 mm^2, see Table 1.

Results and discusion

Figure 1 presents the steps of the analytical fODF reconstruction method. Figure 2 displays the computed fiber ODFs (top) from the 3D-PLI high-resolution data up to the relatively low diffusion MRI resolution, with the corresponding streamlines (bottom). From (A) to (D), the spatial resolution decreases and some streamlines are lost in (D) due to the down-sampling. However the integrity of the brain fiber pathways are preserved by both the fODFs and the streamlines, even at (D) corresponding to dMRI resolution of 1.92 mm^2 in xy-plane and 0.14 mm in the z-axis. We quantify this loss of streamlines by computing their density per voxel at each resolution and figure 3 displays the result. At high resolution, the density map looks more uniform across the tissue slice since, at this level, the super-voxel comprises a single native voxel. As expected, at (B) the density is higher spcefically at main fiber pathways since the scale is still at order of micrometers but tends to go down as the resolution decreases up to the dMRI resolution at (D). Overall, as the resolution decreases, the density of streamlines decreasing too but the fiber pathways are still conserved.

Conclusion

This study presents our analytical fiber ODF reconstruction method and introduces tractography from 3D-Polarized Light Imaging datasets at varying spatial resolutions. By extracting and integrating local fiber directions, we build streamlines which represent the fiber pathways. Results showed brain reconstructed streamlines at different spatial resolutions thanks to the concept of super-voxel. Moreover, they indicate that from the 3D-PLI's micrometer resolution to the diffusion MRI's millimeter resolution, the integrity of the brain fiber pathways is till preserved regardless of the decrease in resolution. This work, therefore, not only opens the door to integration with but also to validation of diffusion MRI tractography across scales in future work.

Acknowledgements

This work was partly supported by ANR "MOSIFAH" under ANR-13-MONU-0009-01, theERC under the European Union's Horizon 2020 research and innovation program (ERC Advanced Grant agreementNo 694665:CoBCoM). We would like to thank professor Marcus Axer and his group for providing the 3D-PLI human brain datasets.

References

1. Jouk et al., "Three-dimensional cartography of the pattern of the myofibres in the second trimester fetal human heart," Anatomy and embryology, vol. 202, no. 2, pp. 103–118, 2000.

2. Axer et al., "A novel approach to the human connectome: ultra-high resolution mapping of fiber tracts in the brain," Neuroimage, vol. 54, no. 2, pp. 1091–1101, 2011.

3. Alimi et al., "Solving the inclination sign ambiguity in three dimensional polarized light imaging with a pde-based method," in Biomedical Imaging (ISBI 2017), 2017 IEEE 14th International Symposium on. IEEE, 2017, pp. 737–740.

4. Axer et al., "Estimating fiber orientation distribution functions in 3D-polarized light imaging," Frontiers in neuroanatomy, vol. 10, 2016.

5. Alimi et al., "Regularizing the ODF estimate with the Laplace-Beltrami operator in 3D Polarized Light Imaging," CoBCoM 2017 - Computational Brain Connectivity Mapping Winter School Workshop, Nov. 2017.

6. Alimi et al., "An analytical fiber odf reconstruction in 3d polarized light imaging," in Biomedical Imaging (ISBI 2018), 2018 IEEE 15th International Symposium on. IEEE, 2018, pp. 1276–1279.

7. Dennis M Healy Jr, Harrie Hendriks, and Peter T Kim, "Spherical deconvolution," Journal of Multivariate Analysis, vol. 67, no. 1, pp. 1–22, 1998.

8. Descoteaux et al., "Regularized, fast, and robust analytical Q-ball imaging," Magnetic resonance in medicine, vol. 58, no. 3, pp. 497–510, 2007.

9. Tournier et al., "Improved probabilistic streamlines tractography by 2nd order integration over fibre orientation distributions," Proceedings of the International Society for Magnetic Resonance in Medicine, 2010, 1670

10. Schmitz et al., "Derivation of fiber orientations from oblique views through human brain sections in 3d- polarized light imaging," Frontiers in Neuroanatomy, vol. 12, pp. 75, 2018.

Figures

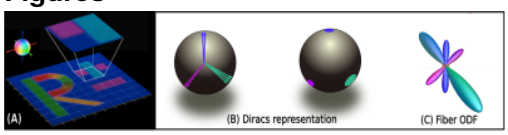

Figure 1: Analytical fiber ODF reconstruction: (A) from [4] , super-voxel definition from high-resolution tissue fiber orientation map, (B) each orientation modeled as Diracs and fiber ODF as weighted sum of these Diracs on the unit sphere, and (C) SH expansion of the fiber ODF in the defined super-voxel.

3D-PLI resolution (μm^3)	Super-voxel size K	dMRI resolution (mm^3)
$64 \times 64 \times 70$	$1 \times 1 \times 1$	$.064 \times .064 \times .07$
	$10 \times 10 \times 2$	$.64 \times .64 \times .14$
	$20 \times 20 \times 2$	$1.30 \times 1.30 \times .14$
	$30 \times 30 \times 2$	$1.92 \times 1.92 \times .14$

Table 1: Imaging spatial resolutions: from 3D-PLI's micrometers to diffusion MRI's millimeters by varying super-voxel dimensions. The tissue coronal section consists of $1000 \times 1700 \times 1$ native voxels.

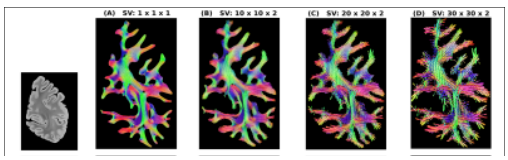

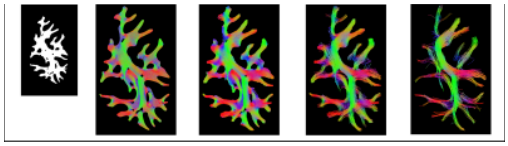

Figure 2: Tractography at multiple spatial scales. From the left, the high resolution tissue slice (top) and the associated white matter mask (bottom). Then up to the right, fiber ODFs (top) and corresponding streamlines (bottom) with increasing super-voxel size up to the dMRI millimeter resolution. SV givess to super-voxel dimensions and local fiber orientations are color-coded (red: left-right, green: posterior-anterior and blue: inferior-superior).

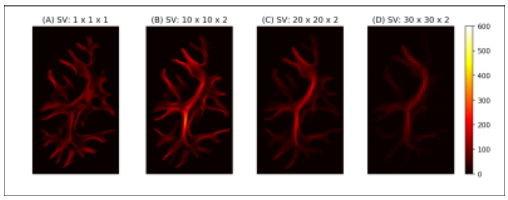

Density maps of streamlines. From 3D-PLI micrometers (A) to diffusion MRI millimeters resolution (D), the density of tracts decreases whereas the fiber pathways are conserved.